Chemistry Proceedings

MDPI

Proceedings

Synthesis and Characterization of Pd over Novel TiO_2 Mixtures: Insights on Metal–Support Interactions †

Matías G. Rinaudo [1,*], Ana M. Beltrán [2], María A. Fernández [3], Luis E. Cadús [1] and Maria R. Morales [1]

[1] Facultad de Química, Bioquímica y Farmacia, Instituto de Investigaciones en Tecnología Química (INTEQUI-CONICET), Universidad Nacional de San Luis (UNSL), Almirante Brown 1455, 5700 San Luis, Argentina; luiscadus@gmail.com (L.E.C.); mrmorale14@gmail.com (M.R.M.)

[2] Departamento de Ingeniería y Ciencia de los Materiales y del Transporte, Escuela Politécnica Superior, Universidad de Sevilla, Virgen de África 7, 41011 Sevilla, Spain; abeltran3@us.es

[3] Instituto de Ciencia de Materiales de Sevilla, CSIC-Universidad de Sevilla, Avda. Américo Vespucio 49, 41092 Sevilla, Spain; asuncion@icmse.csic.es

* Correspondence: matirinaudo@gmail.com

† Presented at the First International Electronic Conference on Catalysis Sciences, 10–30 November 2020; Available online: https://eccs2020.sciforum.net.

Published: 9 November 2020

Abstract: Palladium nanoparticles were supported on unusual mixtures of anatase, TiO_2 (II) and rutile titania phases by wet impregnation, obtaining catalysts with metal contents of ca. 0.25 wt % labeled Pd/Ti5, Pd/Ti45, and Pd/Ti120. Crystalline structures were confirmed by X-ray diffraction. Pd particle sizes in the range of 4–20 nm were observed by scanning-transmission electron Microscopy. External surface areas (S_{BET}) in the range 10–17 $m^2\ g^{-1}$ were higher enough to achieve a good distribution of palladium over titanium oxide outer surface, as evidenced by energy-dispersive X-ray spectroscopy elemental profiles. $Pd^0/Pd^{\delta+}$ atomic ratio measured by X-ray photoelectron spectroscopy showed a decrease from Pd/Ti5 to Pd/Ti120, in line with the decrease in anatase phase present in the catalysts. This behavior suggested that palladium tended to form more $TiPd_xO$ structures in Pd/Ti5 whilst PdO_x structures were more likely to be present on supports with greater amounts of TiO_2 (II) and rutile, due to the distinct metal–support interactions. An increase in reducibility and oxygen mobility from Pd/Ti5 to Pd/Ti120 was observed by temperature programmed measurements and associated to the different high-energy ball milled supports. Catalysts with improved properties reported herein could exhibit an excellent performance in oxidation reactions, e.g., glycerol selective oxidation.

Keywords: titanium oxide; palladium catalyst; metal–support interactions; support effect; redox properties

1. Introduction

Palladium-based catalysts have been extensively used in oxidation reactions, where both dispersion and particle size of metal are considered the dominant factors for a good activity and selectivity [1,2]. However, the role of supports is not limited to be carriers for metal particles [3,4]. Several times, the interface between metal and support is a better active site than the metal itself and thus, an appropriate selection of a catalyst support could reduce the amount of expensive metals needed (e.g., noble metals) [3,5,6]. Moreover, metal–support interaction is a well-known phenomenon attributed to electronic and geometric effects that induce charge transfer between metal particles and support [5,7]. These interactions might not only enhance the adsorption capacity of active sites but also inhibit the sintering of metal particles during reaction [4]. A rational design is

therefore crucial to obtain sustainable metal-supported catalyst with high activity, reusability, and low rate of deactivation [3,7].

TiO_2 is a recognized support for metals, which shows different properties depending on the polymorphs present [3]. Since most reactions in heterogeneous catalysis take place on the surface of metal active phase or the interface between metal and support, the presence of various crystalline phases could enhance catalytic properties [3,8]. To the best of our knowledge, catalysts with modified TiO_2 supports formed by defective structures and unusual polymorphic mixtures have not been used for oxidation reactions until now. Therefore, we propose the study of Pd catalysts supported on novel mixtures of anatase, TiO_2 (II) and rutile (not commercially available) obtained by high-energy ball milling in our previous work [9] to evaluate the different metal–support interactions and their potential role in liquid-phase glycerol selective oxidation.

2. Materials and Methods

2.1. Catalysts Preparation

Wet impregnation method was used to deposit palladium on three different TiO_2 supports obtained in our previous work [9]. Aqueous solutions of HCl with appropriate amounts of $PdCl_2$ (99.99%, Sigma Aldrich, Buenos Aires, Argentina) were added to titania supports in order to achieve palladium loadings of 0.25 wt % on a metal basis. Recovered solids were dried in an oven under vacuum at 70 °C overnight. Then, samples were calcined in a muffle furnace under air at 500 °C for 4 h using a heating ramp of 10 °C min^{-1} to eliminate the rests of metal precursor. Final Pd supported catalysts were labeled Pd/Ti_x, where x corresponds to the milling time of previously synthesized supports.

2.2. Characterization

Catalysts were characterized by means of X-ray diffraction (XRD), scanning-transmission electron microscopy (STEM), energy-dispersive X-ray spectroscopy (EDS), Brunauer–Emmet–Teller (BET) method, inductively coupled plasma–optical emission spectroscopy (ICP-OES), scanning electron microscopy (SEM), X-ray photoelectron spectroscopy (XPS), and temperature programmed measurements (TPM).

3. Results and Discussion

XRD analysis was performed to evaluate the crystalline structure of supported catalysts. We observed (Figure 1A) that samples were formed of different mixtures of titania polymorphs. Pd/Ti5 showed intense reflections associated to anatase phase (PDF 00-21-1272) but also two broad and low-intensity reflections at 27.54 ° and 31.53 ° attributed to (110) rutile reflection (PDF 00-21-1276) and (111) high-pressure TiO_2 (II) reflection (PDF 00-72-0021), respectively. These observations confirmed the presence of an almost pure anatase phase in this catalyst, as expected for its support [9]. On the other hand, Pd/Ti45 exhibited an increase in both TiO_2 (II) and rutile reflections but a decrease in anatase reflections. Pd/Ti120 also showed the reflection attributed to TiO_2 (II) phase and the appearance of several high-intensity rutile reflections. An incipient signal of (101) PdO reflection (PDF 01-06-0515) at 34.04° was detected in Pd/Ti5 catalyst. This behavior suggested the presence of larger palladium crystallites deposited on this catalyst, as also confirmed in further TEM analysis. The absence of this signal in Pd/Ti45 and Pd/Ti120 catalysts could be associated to smaller particles finely dispersed on the supports favored by the greater number of defects and the interfaces between polymorphs present in these supports and under the detection limit of the equipment [9,10].

We also made a rough calculation of the average crystallite size of catalysts by means of Scherrer equation and the relative intensities of the most intense titania reflections of each crystalline phase, (101) anatase, (110) rutile, and (111) TiO_2 (II), as suggested by Dulian et al. [11]. We observed (Table 1) a reduction trend according to the extent of milling in the supports, which is in line with the particle refinement caused by milling process [9,12]. These results were also in line with the increase in S_{BET} values (Table 1) observed in a further analysis. We estimated the catalysts composition using the most

intense Bragg reflections of each titania phase and the equations reported by Duvarci et al. [13], obtaining the unusual mixtures of titania phases (not commercially available) present in the supports (Table 1).

STEM and EDS analyses were carried out to have an insight on the size of palladium species. We could observe Pd particles of 20 nm in Pd/Ti5 catalyst (Figure 1B) and in the range 4–6 and 5–10 nm for Pd/Ti45 and Pd/Ti120 respectively (figures not shown). These observations sustained previous XRD results, where PdO reflection could only be seen in Pd/Ti5 catalyst due to the bigger size of palladium particles. We also made a rough estimation of palladium dispersion by means of the equations provided by Mahata et al. [14] and the average sizes of palladium particles, obtaining values of 6%, 22%, and 15% of metal dispersion for Pd/Ti5, Pd/Ti45, and Pd/Ti120 respectively.

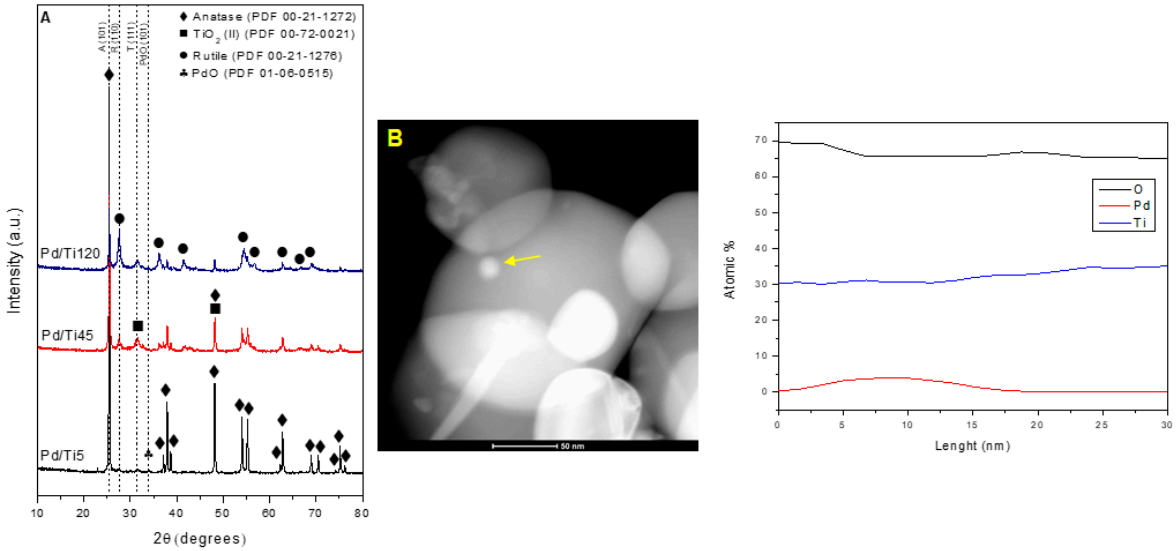

Figure 1. XRD spectra of catalysts (**A**) and STEM image and EDS analysis of Pd/Ti5 sample (**B**).

From textural analyses, we observed specific surface area (S_{BET}) values (Table 1) in accordance with the milling time of each titania support. It is noteworthy that these surface areas were lower than typical values for metals supported on reducible oxides (at least 50 $m^2\ g^{-1}$). However, the small amounts of palladium used during preparation (0.25 wt %) and the enhanced titania supports allowed a good metal dispersion, as observed by STEM-EDS previous analysis. Pore diameters varied in the range 9–21 nm and total pore volumes located in the range 0.04–0.1 $cm^3\ g^{-1}$ (Table 1) as expected for the low porosity of titania [8]. It is important to highlight that pore diameters obtained are higher enough to avoid internal diffusion limitations of big reactant molecules, such as glycerol (average molecule size of 0.62 nm) [15]. Furthermore, the low porosities observed may indicate that S_{BET} values corresponded almost entirely to external surface area [6,9]. This fact could induce the preferential location of palladium species on the external surface of supports, favoring the access of reactants to start the mechanism of reaction [6].

Table 1. Weight fraction (%) of titania polymorphs, average crystallite size, and textural properties of the catalysts.

Catalyst	Anatase wt %	TiO_2 (II) wt %	Rutile wt %	Avg Crystallite Size (nm)	S_{BET} ($m^2\ g^{-1}$)	Pore Diameter (nm) [a]	Total Pore Volume ($cm^3\ g^{-1}$) [b]
Pd/Ti5	99.2	0.3	0.5	54	10	21	0.05
Pd/Ti45	48.4	43.3	8.3	44	15	26	0.1
Pd/Ti120	23	49.4	27.6	42	17	9	0.04

[a] BJH adsorption branch average pore diameter. [b] Quantity of N_2 adsorbed at relative pressure of 0.98.

Morphology of catalysts was studied by SEM (micrographs not shown). Sample Pd/Ti5 showed particles with spherical shape and diameters between 120–220 nm and Pd/Ti45 catalyst presented grape-like clusters formed by a couple of particles, with average diameters between 100–200 nm. Observed agglomeration might be a consequence of electrostatic effects on fine particles (with increased surface energy) as reported by other authors [16]. Smaller sizes were found in case of Pd/Ti120 within a range between 80–180 nm. Moreover, the smaller particle sizes correlated well with the increase in S_{BET} values (Table 1) from Pd/Ti5 to Pd/Ti120.

Pd loadings measured by ICP-OES were found to be in the range 0.2–0.36 wt % compared to the theoretical 0.25 wt %. Differences were attributed to experimental errors during synthesis and/or digestion of the samples.

Surface oxidation state and metal–support interactions were studied by means of XPS (Table 2). At the Ti 2p level we found Ti $2p_{3/2}$ and Ti $2p_{1/2}$ doublets normally located at binding energies of 458.3 and 464 eV and attributed to Ti^{4+} [9]. No signals associated to Ti^{3+} were observed. XPS spectra of O 1s were deconvoluted into two signals (ca. 529.4 and 530.1 eV) associated to lattice oxygen (O_{lat}) and oxygen adsorbed in oxygen vacancies (O_{ads}) respectively [17]. The contents of oxygen vacancies $O_{ads}/(O_{lat} + O_{ads})$ were in the same order as observed in the supports, with a slight variation due to palladium impregnation and further calcination [9]. These low values were previously explained by the migration of oxygen vacancies from the surface to the bulk in order to achieve polymorphic transformation during the synthesis of supports [9].

Table 2. XPS analysis of catalysts

Catalyst	Binding Energy (eV)						at%, XPS		
	Ti $2p_{3/2}$	Ti $2p_{1/2}$	O 1s (O_{lat})	O 1s (O_{ads})	Pd $3d_{5/2}$ (Pd^0)	Pd $3d_{5/2}$ ($Pd^{\delta+}$)	$Pd^0/Pd^{\delta+}$	$O_{ads}/(O_{lat} + O_{ads})$	Pd/Ti
Pd/Ti5	458.81	464.47	529.75	531.24	334.68	336.62	64.45	13.76	0.39
Pd/Ti45	458.4	464.05	529.65	531.29	334.28	336.42	50.2	9.48	0.51
Pd/Ti120	458.35	464	529.59	531.15	334.62	336.32	30.55	10.93	0.64

At the Pd 3d level we observed Pd $3d_{5/2}$ and Pd $3d_{3/2}$ doublets which were deconvoluted into four peaks. We selected Pd $3d_{5/2}$ signals for the interpretation of palladium oxidation state (Table 2). It is well-known that Pd $3d_{5/2}$ level binding energy for Pd^0 is around 335.2 eV [2,6]. Signals with positive shifts respect to the Pd^0 signal are associated to cationic species ($Pd^{\delta+}$ with $\delta \geq 2$) and/or Pd/PdO_x interfaces, while negative shifts are attributed to anionic species and structures such as $TiPd_xO$, where palladium state could be more negative than zero [6]. $Pd^0/Pd^{\delta+}$ atomic ratio (Table 2) showed a decrease from Pd/Ti5 to Pd/Ti120, in line with the decrease in anatase phase present in the catalysts. This behavior could be explained by the greater number of defects and oxygen mobility in the supports milled for longer time, that would lead to electron-deficient palladium species due to the transfer of electron density from palladium to titanium [1,2,4]. Pd/Ti at % were in all cases higher than the theoretical calculation for the bulk (0.19 at %), which confirmed the good dispersion of Pd on the external surface of supports [3].

H_2-TPR measurements were performed to further study metal–support interactions and redox properties of catalysts. Signals observed at around 52 °C (Figure 2A) in all catalyst were associated to the formation of β-PdH_x species on surface metallic palladium, that takes place under reduction at ambient temperature [6]. Negative signals observed at around 72 °C were attributed to the decomposition of formed hydrides, releasing the H_2 [1]. The broad reduction signal with a maximum at 260 °C and the shoulder at 138 °C observed in this catalyst was associated to the reduction of PdO strongly interacting with the titania support [18]. In case of Pd/Ti45 and Pd/Ti120, well-defined signals at 141 °C and 160 °C (respectively) were attributed to the enhanced reduction of PdO species. This increase in reducibility, was related to the greater number of defects, lattice oxygen mobility, and amount of PdO_x species present in the catalysts [1]. Strong signals found in the range 533–578 °C were ascribed to the reduction of surface TiO_2 particles, as observed previously in the supports [9]. Pd/Ti120 also showed shoulders at 307 °C and 558 °C which could be associated to the reduction of

Ti^{4+} species located in defective structures of the polymorphs, due to the longer extent of milling of this catalyst support [9].

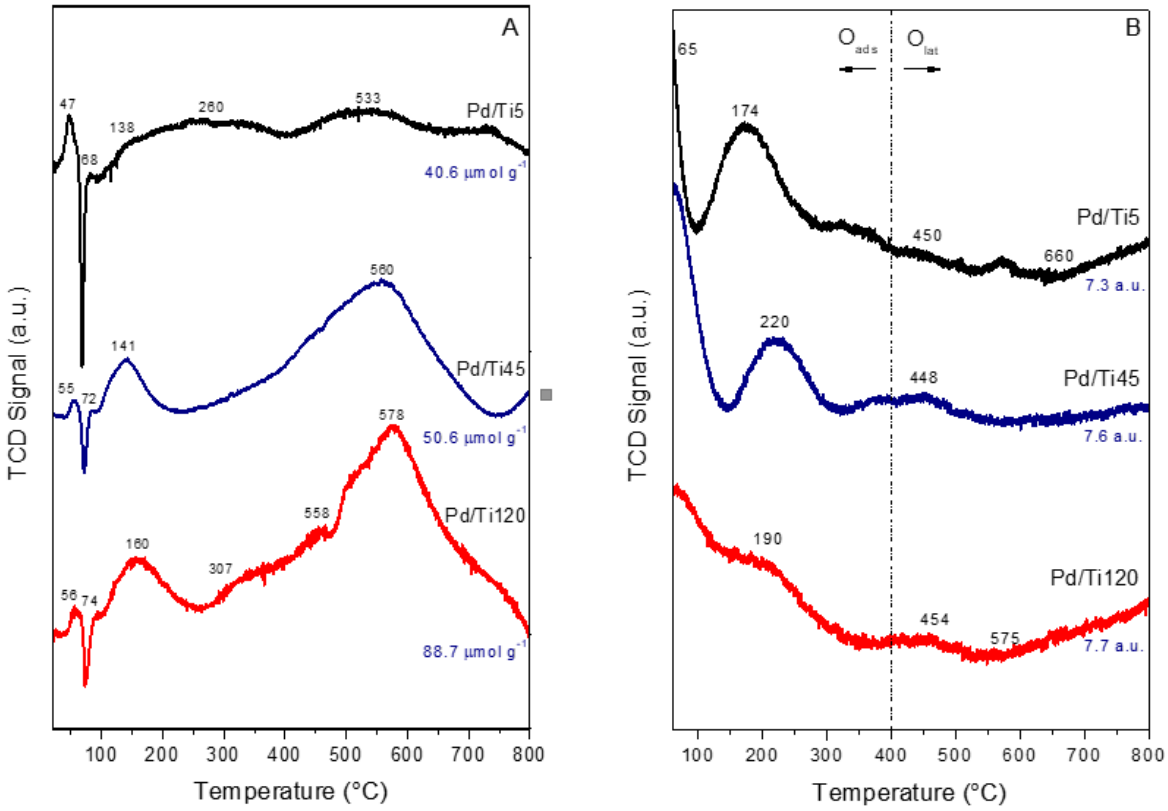

Figure 2. H_2–TPR (**A**) and O_2–TPD (**B**) of catalysts.

H_2-uptakes (Figure 2A) increased from Pd/Ti5 to Pd/Ti120. This behavior was expected due to the longer milling time of the supports, which generates structures with improved oxygen diffusion and reducibility [9].

We performed O_2-TPD measurements (Figure 2B) to obtain information regarding oxygen mobility in the catalysts. Desorption signals found below 100 °C were related to oxygen species weakly bonded to the surface, as reported by other authors [19]. Signals in the range 174–220 °C were attributed to oxygen species adsorbed on oxygen vacancies [19]. Furthermore, signals around 450 °C were ascribed to surface lattice oxygen while desorption peaks above 500 °C were associated to bulk lattice-oxygen release [19]. Well-defined signals observed in case of Pd/Ti45 and Pd/Ti120 catalysts, with more cationic species, were related to the desorption of more active-oxygen species from the surface of its more defective supports [9]. Weight-corrected areas (Figure 2 B) followed the same trend as H_2 uptakes, increasing from Pd/Ti5 to Pd/Ti120. This fact could be ascribed to the greater amount of PdO_x species present in these catalysts, in line with our previous XPS and H_2-TPR analyses.

4. Conclusions

Pd-based catalysts reported in this work showed distinctive properties associated to the unusual mixtures of titania phases present in the supports, previously prepared by high-energy ball milling [9]. Metal nanoparticles were well dispersed on the outer surface of TiO_2, as confirmed by XPS and STEM-EDS analyses. Pd/Ti5 tended to form more anionic Pd species in the form of $TiPd_xO$ structures, which seemed to be less exposed on the surface due to strong interaction with the support, whilst Pd/Ti45 and mainly Pd/Ti120 formed more cationic PdO_x species located on the surface of catalysts, as observed by XPS measurements. In the case of glycerol oxidation, cationic species of palladium would benefit the adsorption of hydroxides and successive glycerol deprotonation, accelerating the mechanism of reaction. Achieved metal–support interactions could improve redox properties,

inducing low-temperature reducibility and an increase in the mobility of reactive oxygen species, as evidenced by TPM analyses, factors well-known to benefit oxidation reactions. Present catalysts are being tested in liquid-phase glycerol selective oxidation in order to study the influence of metal–support interactions on the catalytic performance.

Author Contributions: Conceptualization, M.G.R., M.R.M., and L.E.C.; Investigation, M.G.R.; Visualization, M.G.R.; Writing–original draft, M.G.R.; Writing–review, M.G.R., A.M.B., M.A.F., L.E.C., and M.R.M.; Writing–editing, M.G.R.; TEM measurements and analysis, A.M.B. and M.A.F.; Validation, L.E.C. and M.R.M.; Supervision, L.E.C. and M.R.M.; Resources, M.R.M. All authors have read and agreed to the published version of the manuscript.

Funding: The authors acknowledge the Universidad Nacional de San Luis (UNSL), Agencia Nacional de Promoción Científica y Tecnológica (ANPCyT) and Consejo Nacional de Investigaciones Científicas y Técnicas (CONICET) for their financial support. Also, thanks are given to ANPCyT for the purchase of the SPECS multitechnique analysis instrument (PME8-2003) where XPS analyses were made. The authors also acknowledge the Spanish Ministry of Science, Innovation and Universities, cofinanced by EU FEDER funds, under grant RTI2018-093871-B-I00; the University of Seville for the use of its general research service (CITIUS); the CSIC support under grant PIE-201760E002; and the use of the LANE (ICMS) facilities for TEM data analysis.

Conflicts of Interest: The authors declare no conflict of interest.

References

1. Zhu: J.; Mu, W.; Su, L.; Li, X.; Guo, Y.; Zhang, S.; Li, Z. Al-doped TiO_2 mesoporous material supported Pd with enhanced catalytic activity for complete oxidation of ethanol. *J. Solid State Chem.* **2017**, *248*, 142–149, doi:10.1016/j.jssc.2017.01.028.
2. Dodson, J.J.; Hagelin-Weaver, H.E. Effect of titania structure on palladium oxide catalysts in the oxidative coupling of 4-methylpyridine. *J. Mol. Catal. A Chem.* **2015**, *410*, 271–279, doi:10.1016/j.molcata.2015.09.014.
3. Kim, A.; Sanchez, C.; Patriarche, G.; Ersen, O.; Moldovan, S.; Wisnet, A.; Sassoye, C.; Debecker, D.P. Selective CO_2 methanation on Ru/TiO_2 catalysts: unravelling the decisive role of the TiO_2 support crystal structure. *Catal. Sci. Technol.* **2016**, *6*, 8117–8128, doi:10.1039/c6cy01677d.
4. Wang, N.; Li, S.; Zong, Y.; Yao, Q.; Zhang, Y. Flame synthesis of novel ternary nanocatalysts Pd/CeO_2TiO_2 with promotional low-temperature catalytic oxidation properties. *Proc. Combust. Inst.* **2017**, *36*, 1029–1036, doi:10.1016/j.proci.2016.08.060.
5. Oi, L.E.; Choo, M.-Y.; Lee, H.V.; Ong, H.C.; Hamid, S.B.A.; Juan, J.C. Recent advances of titanium dioxide (TiO2) for green organic synthesis. *RSC Adv.* **2016**, *6*, 108741–108754, doi:10.1039/c6ra22894a.
6. Namdeo, A.; Mahajani, S.; Suresh, A. Palladium catalysed oxidation of glycerol—Effect of catalyst support. *J. Mol. Catal. A Chem.* **2016**, *421*, 45–56, doi:10.1016/j.molcata.2016.05.008.
7. Cui, W.; Li, S.; Wang, D.; Deng, Y.; Chen, Y. High reactivity and sintering resistance of CH_4 oxidation over modified Pd/Al_2O_3. *Catal. Commun.* **2019**, *119*, 86–90, doi:10.1016/j.catcom.2018.10.028.
8. Rui, Z.; Wu, S.; Peng, C.; Ji, H. Comparison of TiO_2 Degussa P25 with anatase and rutile crystalline phases for methane combustion. *Chem. Eng. J.* **2014**, *243*, 254–264, doi:10.1016/j.cej.2014.01.010.
9. Rinaudo, M.; Beltrán, A.M.; I Fernandez, A.; Cadús, L.; Morales, M. Tailoring materials by high-energy ball milling: TiO_2 mixtures for catalyst support application. *Mater. Today Chem.* **2020**, *17*, 100340, doi:10.1016/j.mtchem.2020.100340.
10. Luo, Z.; Kriz, D.A.; Miao, R.; Kuo, C.-H.; Zhong, W.; Guild, C.; He, J.; Willis, B.; Dang, Y.; Suib, S.L.; et al. TiO_2 Supported gold–palladium catalyst for effective syngas production from methane partial oxidation. *Appl. Catal. A Gen.* **2018**, *554*, 54–63, doi:10.1016/j.apcata.2018.01.020.
11. Dulian, P.; Buras, M.; Żukowski, W. Modyfication of photocatalytic properties of titanium dioxide by mechanochemical method. *Pol. J. Chem. Technol.* **2016**, *18*, 68–71, doi:10.1515/pjct-2016-0061.
12. Dutta, H.M.; Lee, Y.-C.; Pradhan, S. Microstructure characterization and polymorphic transformation kinetic study of ball-milled nanocrystalline a-TiO_2–20mol% m-ZrO_2 mixture by X-ray diffraction and electron microscopy. *Phys. E: Low-Dimens. Syst. Nanostruct.* **2007**, *36*, 17–27, doi:10.1016/j.physe.2006.07.042.
13. Duvarcı, Ö.Ç.; Çiftçioğlu, M. Preparation and characterization of nanocrystalline titania powders by sonochemical synthesis. *Powder Technol.* **2012**, *228*, 231–240, doi:10.1016/j.powtec.2012.05.022.

14. Mahata, N.; Vishwanathan, V. Influence of Palladium Precursors on Structural Properties and Phenol Hydrogenation Characteristics of Supported Palladium Catalysts. *J. Catal.* **2000**, *196*, 262–270, doi:10.1006/jcat.2000.3041.
15. Hu, W.; Knight, D.; Lowry, B.; Varma, A. Selective Oxidation of Glycerol to Dihydroxyacetone over Pt−Bi/C Catalyst: Optimization of Catalyst and Reaction Conditions. *Ind. Eng. Chem. Res.* **2010**, *49*, 10876–10882, doi:10.1021/ie1005096.
16. Ali, M. Transformation and Powder Characteristics of TiO_2 during High Energy Milling. *J. Ceram. Process. Res*. **2014**, *15*, 290–293. Available online: http://www.jcpr.or.kr/journal/archive/view/1575 (accessed on 4 December 2020).
17. Yao, X.; Zhao, R.; Chen, L.; Du, J.; Tao, C.; Yang, F.; Dong, L. Selective catalytic reduction of NO_x by NH_3 over CeO_2 supported on TiO_2: Comparison of anatase, brookite, and rutile. *Appl. Catal. B Environ.* **2017**, *208*, 82–93, doi:10.1016/j.apcatb.2017.02.060.
18. Gong, T.; Huang, Y.; Qin, L.; Zhang, W.; Li, J.; Hui, L.; Feng, H. Atomic layer deposited Palladium nanoparticle catalysts supported on Titanium dioxide modified MCM-41 for selective hydrogenation of acetylene. *Appl. Surf. Sci.* **2019**, *495*, 143495, doi:10.1016/j.apsusc.2019.07.237.
19. Yang, X.; Ma, X.; Yu, X.; Ge, M. Exploration of strong metal–support interaction in zirconia supported catalysts for toluene oxidation. *Appl. Catal. B Environ.* **2020**, *263*, 118355, doi:10.1016/j.apcatb.2019.118355.